Environmental Science & Technology

pubs.acs.org/est

Article

Bacterial Diversity Controls Transformation of Wastewater-Derived Organic Contaminants in River-Simulating Flumes

Malte Posselt,[△] Jonas Mechelke,[△] Cyrus Rutere,[△] Claudia Coll, Anna Jaeger, Muhammad Raza, Karin Meinikmann, Stefan Krause, Anna Sobek, Jörg Lewandowski, Marcus A. Horn,[*,◇] Juliane Hollender,[*,◇] and Jonathan P. Benskin[*,◇]

Cite This: *Environ. Sci. Technol.* 2020, 54, 5467−5479

Read Online

ACCESS | Metrics & More | Article Recommendations | Supporting Information

ABSTRACT: Hyporheic zones are the water-saturated flow-through subsurfaces of rivers which are characterized by the simultaneous occurrence of multiple physical, biological, and chemical processes. Two factors playing a role in the hyporheic attenuation of organic contaminants are sediment bedforms (a major driver of hyporheic exchange) and the composition of the sediment microbial community. How these factors act on the diverse range of organic contaminants encountered downstream from wastewater treatment plants is not well understood. To address this knowledge gap, we investigated dissipation half-lives (DT50s) of 31 substances (mainly pharmaceuticals) under different combinations of bacterial diversity and bedform-induced hyporheic flow using 20 recirculating flumes in a central composite face factorial design. By combining small-volume pore water sampling, targeted analysis, and suspect screening, along with quantitative real-time PCR and time-resolved amplicon Illumina MiSeq sequencing, we determined a comprehensive set of DT50s, associated bacterial communities, and microbial transformation products. The resulting DT50s of parent compounds ranged from 0.5 (fluoxetine) to 306 days (carbamazepine), with 20 substances responding significantly to bacterial diversity and four to both diversity and hyporheic flow. Bacterial taxa that were associated with biodegradation included Acidobacteria (groups 6, 17, and 22), Actinobacteria (*Nocardioides* and *Illumatobacter*), Bacteroidetes (*Terrimonas* and *Flavobacterium*) and diverse Proteobacteria (Pseudomonadaceae, Sphingomonadaceae, and Xanthomonadaceae). Notable were the formation of valsartan acid from irbesartan and valsartan, the persistence of *N*-desmethylvenlafaxine across all treatments, and the identification of biuret as a novel transformation product of metformin. Twelve additional target transformation products were identified, which were persistent in either pore or surface water of at least one treatment, indicating their environmental relevance.

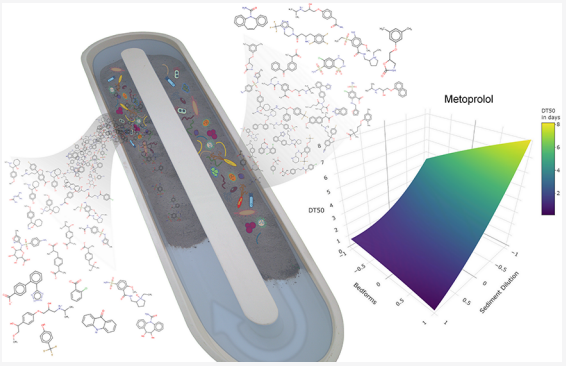

1. INTRODUCTION

The design of conventional wastewater treatment plants (WWTPs) is considered inefficient for the removal of organic contaminants present in wastewater. In particular, polar organic contaminants such as pharmaceuticals and personal care products tend to be only partially removed or pass the treatment process unchanged,[1] leading to the discharge of a complex mixture of substances into surface waters. Hyporheic zones, which form the water-saturated flow-through sediments of rivers, are often considered the last line of defense for preventing wastewater-derived organic contaminants from reaching near-surface aquifers that are used for drinking water production. Moreover, hyporheic zones are adjudged an essential role in the self-purification of streams, as the interplay of complex physical, chemical, and biological processes creates ideal conditions for organic matter decomposition, nutrient cycling, and biotransformation of contaminants.[2,3] The sediments provide a large surface area for biofilms with diverse microbial communities, which contribute substantially to global biogeochemical fluxes.[4] Fungi and other microeukaryotes are part of the microbial community in streams, although rare relative to bacteria, and potentially contribute to biodegradation processes. Eukaryotic algae may form biofilms together with bacteria in the benthic zone; however, their occurrence in sediments is highly limited by the low availability of light. Archaea likewise represent only a minor fraction of the stream bed microbial community and are restricted to specialized niches in the hyporheic zone. Thus, it is not surprising that hyporheic zone biofilms are dominated by bacteria.[4−6] The varying redox conditions along many hyporheic flowpaths render the hyporheic zone an efficient

Received: November 15, 2019
Revised: March 21, 2020
Accepted: April 6, 2020
Published: April 6, 2020

https://dx.doi.org/10.1021/acs.est.9b06928
Environ. Sci. Technol. 2020, 54, 5467−5479

(bio)reactor for a multitude of transformation processes. This is why compounds that are particularly sensitive to certain redox conditions are expected to degrade faster in an environment that promotes hyporheic exchange, ideally enabled by a broad distribution of hyporheic residence times.[3,7]

Despite a growing number of studies in both the laboratory[8−11] and field[12−14] highlighting the important role of sediments in the degradation of contaminants, few studies have focused on processes occurring in hyporheic zones[2,3,15−18] and even fewer on transformation products (TPs) formed in hyporheic zones. TPs may be more biologically active,[19,20] persistent,[21,22] mobile,[23] and abundant[24] in the environment in comparison to the corresponding parent, yet they are often overlooked due to a lack of reference standards. With the emergence of suspect and nontarget screening workflows employing high-resolution mass spectrometry, tentative identification of suspected or unknown TPs without the use of reference standards is possible.[25,26] However, few studies have made use of suspect[18] or nontarget[27] approaches to study the occurrence or biodegradation of contaminants in hyporheic zones. This is an important area of investigation, since biodegradation is considered more efficient in hyporheic zones than in WWTPs, owing to longer residence times[27] and higher microbial diversity in hyporheic zones,[15] which ultimately may increase adaptation and metabolic process rates.[28] Moreover, hyporheic exchange flows (HEFs) facilitate contact between contaminants in surface water and potential microbial degraders. HEF as a function of hydraulic conductivity and sediment morphology,[29] together with the resident microbial community structure (especially diversity)[30] are therefore potential key controls of the fate of organic contaminants in lotic aquatic environments. Although long hypothesized, such links were never systematically addressed.

The goal of this study was to evaluate the influence of bacterial taxonomic diversity and HEF on the dissipation half-lives (DT50s) of organic contaminants detected in surface waters and the associated formation of TPs. The experiment was performed following a central composite face factorial design using 20 flume mesocosms, as reported elsewhere.[31] We used taxonomic diversity as a proxy for biodegradation capacity due to limited information on the functional diversity of most bacterial pollutant degraders and considering the reported positive correlation between taxonomic and functional diversity.[32] The taxonomic diversity in the sediment used in the flume study was manipulated by mixing sterilized sand with a sediment inoculum from the wastewater-impacted river Erpe in Berlin by a dilution to extinction approach.[32] HEF was manipulated by varying the number of sediment bedforms. Thirty-one common organic contaminants found in WWTP effluents were selected, and their dissipation together with the formation of TPs was followed using LC coupled to (high-resolution) mass spectrometry. Time-resolved high-throughput sequence analysis was applied to characterize the biodiversity and identify potential key bacteria driving biotransformation.

2. MATERIALS AND METHODS

Test compounds were selected on the basis of their occurrence at the wastewater-impacted River Erpe (i.e., the location of sediment inoculum collection),[33] frequent detection in aquatic environments, a wide range of physicochemical properties with the majority of compounds being polar (SI.A), and diverse dissipation behaviors (from fast degrading to persistent).[8,11] The 31 test substances (along with their abbreviations) are as follows: ACS, acesulfame; AMI, amisulpride; ATE, atenolol; BENP, benproperine; BEZ, bezafibrate; BNZ, benzotriazole; CBZ, carbamazepine; CEL, celiprolol; CFA, clofibric acid; CIT, citalopram; DIC, diclofenac; FLEC, flecainide; FLX, fluoxetine; FUR, furosemide; GEM, gemfibrozil; HCTZ, hydrochlorothiazide; IBU, ibuprofen; IRB, irbesartan; KET, ketoprofen; METF, metformin; METP, metoprolol; MTX, metaxalone; NPX, naproxen; PAR, paracetamol (3-acetamidophenol); PROP, propranolol; SIT, sitagliptin; SMX, sulfamethoxazole; SOT, sotalol; SUL, sulpiride; VAL, valsartan; VEN, venlafaxine. ACS and CBZ were previously reported along with details of the experimental design and methods[31] and are included here for comparative purposes along with unpublished data on their TPs. Target TPs are denoted by a three-letter code preceded by "TP", suspect TPs by their nominal mass preceded by "sTP" (Table SI.A-3). Further information on standards, and other chemicals used for fortification and chemical analysis are provided in section SI.A in the Supporting Information.

2.1. Experimental Design, Background Parameters, and Sampling Details. The experiment was based on a central composite face factorial design and used 20 circulating flume mesocosms (2 × 0.4 m) simulating different river conditions. Fundamentals of the flume experimental design can be found elsewhere.[27] In brief, the sediment volume was 20 L per flume covered with 60 L deionized water (ReAgent Chemicals, Cheshire, England) and every flume was equipped with a pump (NWA 1.6 adj 2.6 W, Newa Wave Industria, Loreggia, Italy) to establish a surface water flow velocity of ca. 0.08 m s^{-1} similar to the River Erpe (0.05−0.3 m s^{-1}),[33] from which natural sediment inoculum was obtained (details are given in ref 31). Nutrients, such as phosphate and ammonium, and other solutes (inorganic ions in mg L^{-1} range and organic and inorganic micronutrients in μg L^{-1} range (Table S1 in ref 31) were added, resembling concentrations and composition in the natural River Erpe).[33] Two experimental variables (i.e., HEF and bacterial diversity) at three levels each were studied: flume sediments consisted of baked sand (reduced biological activity) inoculated with three different amounts of biologically active sediment collected from the River Erpe, which receives high loads of treated wastewater.[33] The approach was based on the dilution to extinction principle: i.e., the least abundant species in a preceding community were eliminated through sequential dilution, resulting in a less diverse community in comparison to the original community.[32] The level of bacterial diversity was thus expected to decrease in the order S1 (1:10 sediment:sand) > S3 ($1:10^3$ sediment:sand) > S6 ($1:10^6$ sediment:sand). Additionally, the sediment morphology in the flumes was manipulated at three levels to induce different intensities of HEF by varying the number of bedforms (section SI.B).[34] The level of HEF decreased in the order B6 (three bedforms on each side of the flume) > B3 (three bedforms on one side) > B0 (no bedforms). The number of flumes per treatment combination (S and B) in the experimental design was as follows: S1 + B6:2, S3 + B6:2, S6 + B6:2, S1 + B3:2, S3 + B3:4, S6 + B3:2, S1 + B0:2, S3 + B0:2, S6 + B0:2 (Figure SI.B-1). After 12 days of preincubation, the flumes were fortified with 10 μg L^{-1} of each of the 31 test compounds. Many test compounds were found with similar concentrations in the river Erpe, which we aimed to simulate,[17,33] but also in other streams or WWTP effluents.[3,35,36] Two unamended

https://dx.doi.org/10.1021/acs.est.9b06928
Environ. Sci. Technol. 2020, 54, 5467−5479

flumes (S3 + B3) were included as biotic controls and served as a reference for the effect of test compounds on taxa in amended flumes. Surface and pore water were sampled prior to fortification and thereafter on days 1, 2, 3, 7, 14, 21, 28, 42, 47, 56, and 78. Sediment was collected before fortification and after 21 and 56 days. Pore water samplers were installed during bedform formation (details in section SI.B). Two former studies provided experimental[31] and modeled[34] evidence that (a) the two variables, HEF and bacterial diversity, were successfully manipulated at three levels in the central composite face factorial design setup, (b) sediment dilutions translated into different levels of bacterial diversity at a similar bacterial biomass, and (c) HEF increased in the presence of bedforms.

2.2. Chemical Analysis. A total of 242 surface water, 272 pore water, and 72 sediment samples were collected. Water samples were split and analyzed at Stockholm University and the Swiss Federal Institute of Aquatic Science and Technology (Eawag) using direct injection reversed-phase ultrahigh-performance liquid chromatography electrospray ionization triple quadrupole tandem mass spectrometry (RP-UHPLC-ESI-QqQ)[17] and direct injection reversed-phase liquid chromatography electrospray ionization high-resolution tandem mass spectrometry (RP-LC-ESI-HRMS/MS) (sections SI.C−SI.F), respectively. If a target analyte was included in both methods, the data were pooled (section SI.K.a). The two independent analyses increased the analytical robustness and extended the analyte range. QA/QC information, a method comparison and background concentrations are provided in section SI.F. Concentration time trends of target TPs and signal time trends of suspect TPs were investigated visually, and the frequency of target TPs was determined statistically using MetaboAnalyst 3.0.[37] Two-way hierarchical clustering was performed using Euclidean distance as a measure of similarity and clustering using Ward's linkage. The use of HRMS allowed for the screening of suspected biotransformation products, which was conducted with Compound Discoverer (version 2.1, Thermo Scientific; see section SI.C.d). Suspect TPs can be found in Table SI.M-22 and section SI.O together with the confidence level of identification.[38]

2.3. Response Surface Model. Concentrations for a given compound were normalized by dividing by the concentration at $t = 0$ (i.e., c/c_i) prior to averaging values produced by Stockholm University and Eawag. Compounds measured by one method (i.e., Stockholm University or Eawag) were treated in the same manner except for the averaging step. The normalized averaged concentrations of each compound and flume were then fitted to a first-order kinetic degradation curve using the *mkin* package[39] in R.[40] If a lag phase was observed (i.e., an initial period with increase in concentrations or static initial concentrations followed by a degradation phase), the lag-phase time points were removed prior to curve fitting. A two-tailed t test was used to assess if the first-order kinetic constant was significantly different from zero ($p \leq 0.05$), and thereafter DT50s were calculated. For compounds with DT50s for all 20 flumes in the central composite face factorial design, DT50s were used to fit the Response Surface Model (*rsm* package version 2.10[41] in R[40]) with bedforms and sediment dilution as coded variables: $DT50 = \beta_0 + \beta_1 S + \beta_2 B + \beta_3 S{\cdot}B + \beta_4 S^2 + \beta_5 B^2 + \varepsilon$ (with β_1 and β_2 as first order, β_4 and β_5 as second order, and β_3 as interaction terms; details in Table SI.B-6). For CFA, irbesartan, metoprolol, PROP, SIT, and SOT, missing DT50s were imputed (section SI.K.a). The linear and quadratic coefficients of both variables were calculated, and two-tailed t tests were used to determine if the RSM fitted coefficients were statistically different from zero. The significance of the linear and quadratic terms was assessed with an ANOVA. An F test, adjusted, R2 and lack of fit were used to assess the suitability of the model.

2.4. Bacterial Analysis. DNA was extracted from the sediment samples and used to quantify the bacterial community with real-time quantitative PCR of 16S rRNA genes. 16s rRNA gene amplicons were sequenced via the Illumina Miseq amplicon sequencing platform and bacterial community diversity and composition dynamics assessed on the basis of operational taxonomic units (OTUs) defined at 97% similarity. ANOVA was used to compare the α diversity indices between sediment dilution levels (S1, S3, S6, i.e. low, medium and high dilution, resulting in high, medium, and low diversity, respectively) and bedforms (B0, B3, B6), while the *DESeq2* function[42] in R[40] was used to identify potential degraders of test compounds. More details on the DNA extraction and downstream processing can be found in section SI.G.

3. RESULTS AND DISCUSSION

3.1. Effect of Sediment Dilution and Bedforms on Bacterial Gene Copy Numbers and Diversity. Sediment samples collected after 12 days of preincubation reached approximately 1.2×10^6 16S rRNA gene copy numbers per gram sediment dry weight (Table SI.G-10) with no significant differences observed across the sediment dilution levels or bedform numbers (ANOVA, $p > 0.05$). This suggests regrowth of bacterial communities in the different diluted sediment treatments to similar cell densities. However, during the attenuation phase, significantly higher bacterial copy numbers were observed in S1 (low sediment dilution) in comparison to S3 (medium dilution) and S6 (high dilution) at day 56 (ANOVA, $p \leq 0.05$). This may be attributable to the growth of rare slow-growing taxa in the original sediment bacterial community found in the S1 treatment but eliminated in the S3 and S6 treatments through the dilution to extinction approach. Since bacterial abundance was similar between treatments as indicated by qPCR (Table SI.G-10) after the preincubation phase, any differences between treatments are attributed to differences in bacterial diversity rather than overall bacterial abundance for this period. The sediment dilution resulted in a significant decrease in species richness and diversity (Shannon) in S3 and S6 in comparison to S1 at days 0, 21, and 56 (ANOVA, $p \leq 0.05$) and between S6 and S3 at day 56 (Figure 1). Furthermore, a significant decrease in evenness was only observed in S3 and S6 in comparison to S1 at day 56 (ANOVA, $p \leq 0.05$, Figure 1). These results indicated that the dilution to extinction method created a gradient in the bacterial α diversity. The bedform elements did not significantly affect any of the diversity indices measured at any of the sampling time points (ANOVA, $p > 0.05$, Figure 1). This was unexpected, since an increased number of bedforms was postulated to promote HEF that is associated with increased oxygen and nutrient supply,[43] hence promoting higher bacterial community diversity.

3.2. Bacterial Community Structure and Taxa Associated with Test Compound Biotransformation. We detected 17 known phyla in S1 (low sediment dilution) in comparison to 13 known phyla in the S3 (medium dilution)

https://dx.doi.org/10.1021/acs.est.9b06928
Environ. Sci. Technol. 2020, 54, 5467−5479

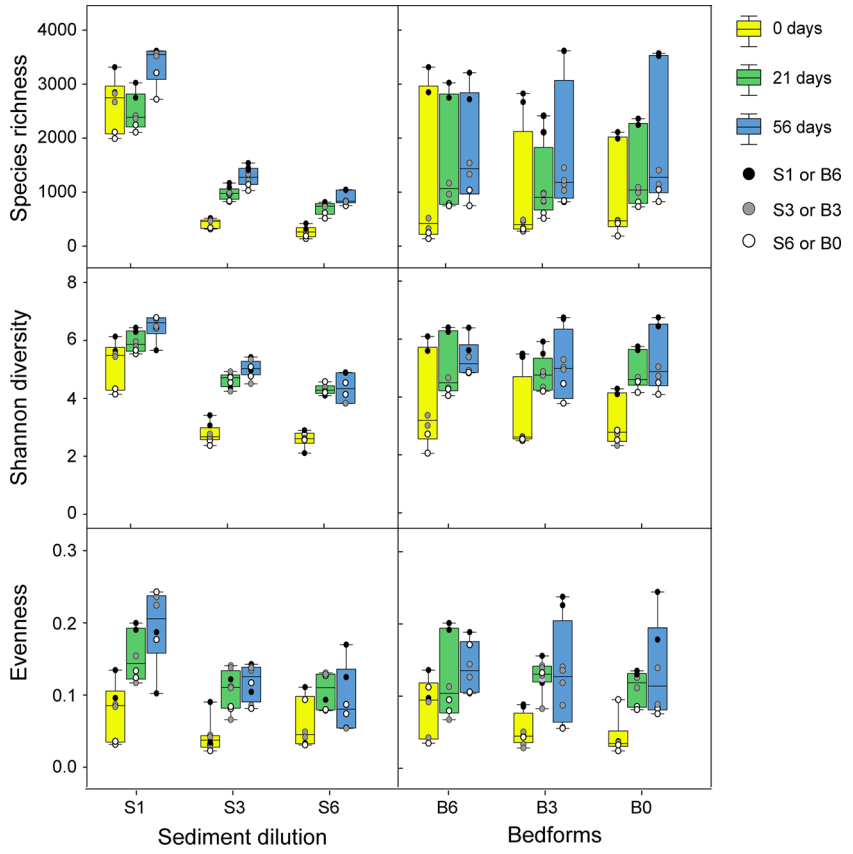

Figure 1. Box plots of α diversity indices based on 16S rRNA gene sequence analysis as a function of sediment dilution and bedform number. S1, S3, and S6 correspond to sediment:sand dilutions of 1:10, $1:10^3$, and $1:10^6$, respectively; B6, B3, and B0 correspond to 6, 3, and 0 bedforms, respectively. Samples were collected before fortification (day 0) and at days 21 and 56 of the attenuation phase. The diversity indices, species richness, and Shannon diversity as a function of sediment dilution were significantly different between the least dilute sediment and the subsequent dilutions at all sampling time points, while evenness was only significantly different between the least diluted sediment and the subsequent dilutions at day 56 ($p \leq 0.05$). Diversity indices among treatments as a function of the bedform number were similar ($p > 0.05$).

and S6 (high dilution) dilution levels (Figure SI.G-5). This shows that the dilution to extinction approach successfully removed some of the rare occurring phyla such as Saccharibacteria, Latescibacteria and Nitrospirae detected in the S1 sediment bacterial community. Within the remaining phyla, specific genera impacted by the presence of test compounds were identified on the basis of a significant change in abundance relative to unamended controls using the *DESeq2* function (Table SI.G-12). Genera associated with the collective biotransformation of the test compounds were considered enriched in the case of $\log_2$ fold change >0 in comparison to unamended samples. Such enrichment suggests that they might include both some pollutant-degrading species along with pollutant-insensitive species. Some of the enriched genera detected in the present study and previously associated with degradation of organic contaminants in diverse environments included operational taxonomic units affiliated with Holophagae and subgroups 6, 17, and 22 in the phylum Acidobacteria, which were associated with polychlorinated biphenyl[44] and petroleum compound degradation.[45] Within the phylum Actinobacteria, genera such as *Nocardioides*, harbor known ibuprofen degraders,[46] while *Illumatobacter* is among genera enriched in the presence of organic pollutants such as anilines and phenols, polycyclic aromatic hydrocarbons, and organochlorine pesticides.[47] Genera of the phylum Bacteroidetes such as *Terrimonas* and *Flavobacterium* that include benzo[*a*]pyrene-[48] and ibuprofen-degrading species were also enriched.[49] The dominant phylum Proteobacteria was represented by several genera, including *Sphingomonas*, *Sphingobium*, and *Novosphingobium* in the family Sphingomonadaceae that is widely characterized as a family with many prolific aerobic degraders of a wide variety of aromatic compounds[50] as well as Comamonadaceae, also aerobic degraders of aromatic compounds.[51] Within the families Xanthomonadaceae and Pseudomonadaceae the genera *Arenimonas* and *Pseudomonas* were enriched in response to the 31 test compounds. These genera have previously been linked to biodegradation of polyaromatic compounds such as naphthalene.[50] The enriched *Mesorhizobium* is closely related to the metformin degrader *Aminobacter*.[52] These genera belong to the family Phyllobacteriaceae, whose other members are known for degradation of micropollutants such as dichlorobenzamide.[53] Most other enriched operational taxonomic units are affiliated with yet to be classified genera and families, which suggests a wide array of taxa potentially involved in the degradation of organic contaminants in hyporheic sediments and highlights the hyporheic zone as a reservoir of hitherto undetected microbial diversity. In contrast, some genera exhibited $\log_2$ fold change <0 in the presence of test compounds relative to unamended controls (Table SI.G-12), indicating a decrease in their abundance likely due to the potential negative effect of the test compounds. Previous studies[47,54] have reported such effects of micropollutants on a certain fraction of the indigenous environmental microbiota.

https://dx.doi.org/10.1021/acs.est.9b06928
Environ. Sci. Technol. 2020, 54, 5467−5479

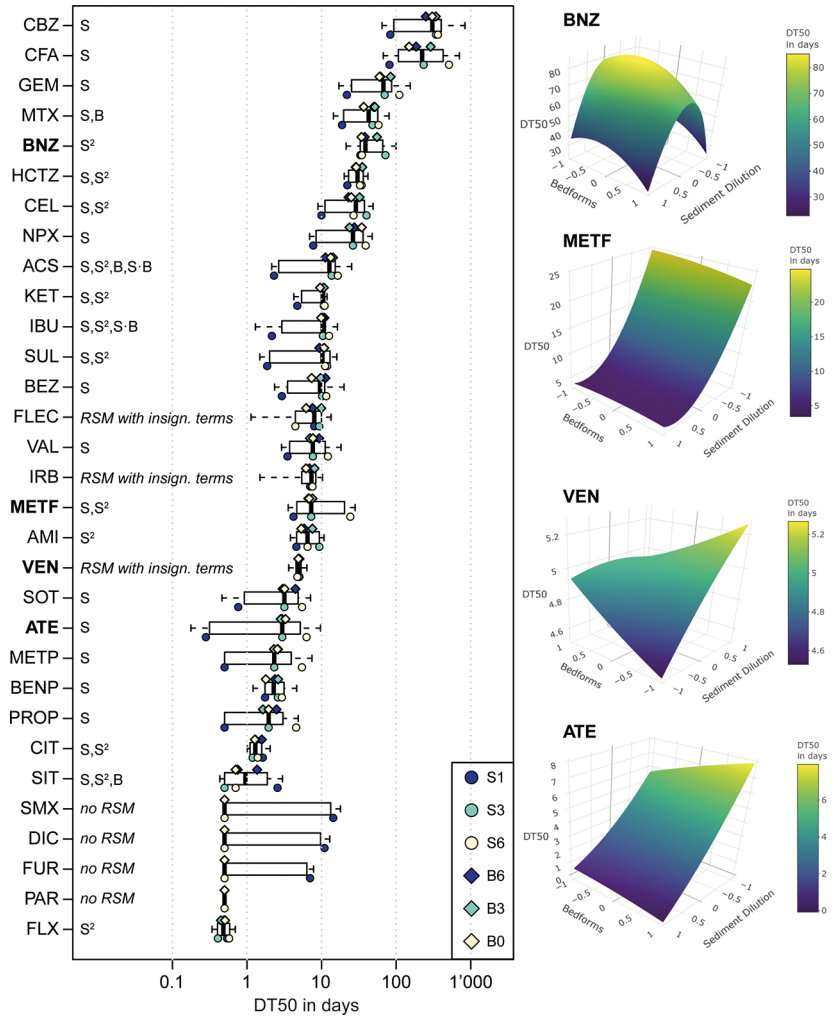

Figure 2. Dissipation half-lives (DT50s) of 31 test (parent) compounds in water-sediment test flumes across different levels of bacterial diversity (as a function of sediment dilution S1 1:10, S3 $1:10^3$, S6 $1:10^6$) and bedform numbers (B6, $n = 6$; B3, $n = 3$; B0, $n = 0$) displayed as box plots (outliers not shown). Previously published CBZ and ACS data are included here for comparison.[31] The response of DT50s toward these variables was evaluated with a response surface model (RSM, examples are shown in the right margin of the figure). Significant linear sediment dilution variable (S), linear bedform variable (B), quadratic sediment dilution variable (S^2), and/or interactive ($S{\cdot}B$) terms in the RSM are indicated right next to the substances. Compounds with insignificant RSM parameters are marked as "*RSM with insignificant terms*" (e.g., VEN) or "*no RSM*" if DT50s were too small to fit the RSM (e.g., SMX).

3.3. Dissipation Half-Lives of Organic Contaminants. Median DT50s of the 31 test compounds ranged from 0.5 (fluoxetine) to 306 days (carbamazepine) (Figure 2 and sections SI.H–SI.J). The most persistent compounds (median DT50s >20 days across all flumes) were carbamazepine (306 days), clofibric acid (223 days), gemfibrozil (67 days), metaxalone (43 days), benzotriazole (39 days), hydrochlorothiazide (30 days), celiprolol (29 days), and naproxen (26 days). In contrast, diclofenac, furosemide, paracetamol, and sulfamethoxazole dissipated in less than 1 day in the majority of the flumes. For these short-lived substances, DT50s and consequently RSMs could not be determined, and instead DT50s of 0.5 day were assumed. Parent compounds with very short DT50s and RSMs were fluoxetine (0.5 days), sitagliptin (1.0 day), and citalopram (1.3 days). Among the spiked substances were five beta-blockers (atenolol, celiprolol, metoprolol, propranolol, and sotalol), four of which had similar DT50s (2.0–3.2 days), while the DT50 for celiprolol was 1 order of magnitude higher (29 days). Celiprolol features a disubstituted urea moiety that might be less prone to biological hydrolysis than, for example, the amide or ether side chain in atenolol or metoprolol, respectively. We attribute the observed dissipation mainly to biodegradation, while photolysis and sorption were likely to play a minor role (section SI.B.a) in the present setup for most compounds (exceptions: irbesartan, some cationic compounds). Due to its low carbon content and the low fraction of fine minerals, the sediment generally was a poor sorbent and the tent covering the flumes prevented direct solar radiation[31] (section SI.B.a). However, cationic exchange at anionic surfaces in the sediment may play a role for cationic compounds such as metoprolol.[55] For some compounds (especially those with high log K_{ow}) sorption may have had an effect due to the presence of biofilms. Nevertheless, since overall bacterial abundances were similar between the diversity levels, potential sorption should have a similar effect on all levels and not affect the model results.

3.4. Response Surface Model to Evaluate the Dissipation of Organic Contaminants. Overall, RSMs were fit to the DT50s of 27 compounds (section SI.K.b). For DIC, FUR, PAR, and SMX, DT50s could not be obtained for

https://dx.doi.org/10.1021/acs.est.9b06928
Environ. Sci. Technol. 2020, 54, 5467–5479

the majority of flumes (see above), and consequently the RSM could not be applied. On the basis of the RSM, sediment dilution and bedform variable explained ∼70% of DT50 variance (derived from adjusted R2s, Table SI.K-17). The best RSM fits were obtained for metformin (96%), IBU (95%), and KET (93%) and the lowest for VEN (5%), irbesartan (10%), and flecainide (17%). For the last three compounds, RSM coefficients (β_x) (cf. section 2.1) were not significantly different from zero (two-sided t test, $p > 0.05$). The remaining 24 compounds featured significant ($p \leq 0.05$) coefficients of the sediment dilution variable (S): linear ($n = 12$), quadratic ($n = 3$), or both ($n = 9$) (Figure 2). For ACE, SIT, and MTX, the linear bedform variable (B) was also signficant for attenuation, and in the case of ACS and IBU, a significant linear interaction of S and B ($S{\cdot}B$) was observed. Except for CFA, all first order (S, B), second order (S^2, B^2) and/or interaction ($S{\cdot}B$) term(s) were significant (ANOVA; $p \leq 0.05$). A lack of fit of the RSM was only observed for ACS.[31] On the basis of the RSM, the test compounds were classified as (1) no response to S and B ($n = 3$), (2) response to S or S^2 and B or $S{\cdot}B$ ($n = 4$), or (3) response to S or S^2 ($n = 20$) (Table SI.K-18). The low correlation between DT50s and the bedform variable is unsurprising. Theoretical HEFs under the initial setup conditions provided by a numerical model were similar for three and six bedforms (11 and 13.6 L day^{-1}) but close to zero (0.4 L day^{-1}) in the absence of bedforms.[34] Because 20 of 27 substances responded only to the sediment variable (i.e., S or S^2), TP discussions in the following sections are only likely to reflect the effects of diversity and will not differentiate between bedform numbers.

3.5. Association between Bacterial Diversity and DT50s. Species richness, Shannon diversity, and evenness as a function of sediment dilution (Figure 1) significantly correlated with 21, 22 and 9 out of the 31 biotransformed compounds, respectively, in comparison to 3, 6, and 6 as a function of the bedform number (Table SI.G-11, Spearman, $p \leq 0.05$). These findings suggest that bacterial communities with higher species richness and diversity are more efficient at transforming a larger number of individual test compounds. Our findings further extend previously reported correlations between bacterial diversity and organic compound biodegradation.[31,32,56]

3.6. Transformation Product Dynamics at Different Levels of Bacterial Diversity and Hyporheic Exchange Flow. In total, we determined 32 TPs in at least one pore water or surface water sample using targeted methods (confidence level 1) and an additional 24 suspected TPs (confidence level 3−4) in surface water via a suspect screening workflow described in section SI.C. For six parent compounds (ACS, FLEC, GEM, NPX, PAR, and SIT) no TPs were included in our target list and suspects were not found. Exclusively target TPs were detected for BNZ, CBZ, CIT, DIC, hydrochlorothiazide, IBU, SMX, SUL, valsartan, and VEN, while only suspect TPs were found for BENP, CEL, CFA, FUR, KET, MTX, PROP, and SOT. Substances to which we could associate both suspect and target TPs were AMI, atenolol, BEZ, FLX, irbesartan, metformin, and metoprolol. Only 5 out of the 32 TPs on our target list could not be quantified in any sample: TP.BEZ4H, TP.CAO, TP.DICHA, TP.IBUC, and TP.MEH. Out of these, the nondetection of α-hydroxymetoprolol (TP.MEH) was the least expected, since it was previously found together with metoprolol acid (MEA) in, for example, pore and surface water of the River Erpe, sometimes at higher concentrations than those for metoprolol acid.[17,33] Three TPs were exclusively detected in pore water (TP.CAI, TP.DAM, and TP.IBU1H), whereas two were specific for surface water (TP.BEZ1H and TP.BZCPA), but all were infrequently detected (<7%; Figure 3).

Among all target TPs, valsartan acid (TP.VAA 20.1 μg L^{-1} pore water, 16.4 μg L^{-1} surface water) and metoprolol acid (15.3 μg L surface water, 14.9 μg L^{-1} pore water) occurred at the highest concentrations. The most abundant TP that formed exclusively from a single parent compound (metformin) was guanylurea (TP.GU) with 9 μg L^{-1} in surface water and 7.1 μg L^{-1} in pore water. Several BNZ TPs occurred in high abundance (1.1−5.6 μg L^{-1}), including 1-hydroxybenzotriazole (TP.BEZ1H), 1-methylbenzotriazole (TP.BEZM), and 4-/5-methylbenzotriazole (TP.BEZ5M) but were at the same time almost exclusively formed in S1 treatments (low dilution, high diversity) and therefore overall not very frequently detected. To our knowledge, TP.BEZ5M has not been described as a TP of BNZ before, but the methylation at the benzene ring was reported as a possible biotransformation reaction of BNZ (more details in section SI.M.f).[57] There is a lack of literature on the occurrence and environmental relevance of benzotriazoles, but our data suggest that these substances and especially their TPs warrant further investigation.

Seven TPs were detected in more than 50% of all analyzed samples: *N*-desmethylvenlafaxine (TP.VND, 77%), 4-amino-6-chloro-1−3-benzenedisulfonamide (TP.ABS, 75%), metoprolol acid (metoprolol acid, 68%), chlorothiazide (TP.CTZ, 66%), valsartan acid (62%), carbamazepine-10,11-epoxide (TP.CEPX, 56%), and venlafaxine *N*-oxide (TP.VNO, 54%). In total, 21 of the detected TPs (11 confidence level 1, 12 confidence level 3−4) displayed increasing or constant concentrations in surface water in at least one of the three diversity groups throughout the experiment (i.e., no signs of degradation) and were therefore considered potentially persistent (Figure 3). Eleven target TPs showed the latter behavior in pore water and seven of those were accumulating or constant in both pore water and surface water (TP.ABS, TP.AMINO, TP.CDH, TP.CEPX, TP.CTZ TP.SMXA, and TP.VND). In these counts we included TPs with increasing trends leveling off toward the end of the experiment, which can be due to depletion of the parent molecules (e.g., TP.CEPX).

In several cases, increasing TP concentrations were observed in dilution levels S3 and/or S6 only (medium and low diversity), while higher bacterial diversity in S1 treatments seemed to enable their degradation (e.g., TP.AMINO). Remarkably, TP.VND was the only TP with increasing or constant concentrations across all diversity levels in both pore water and surface water throughout the experiment, despite the low DT50 of its parent compound (VEN). Accordingly, ∼80% of VEN was removed from the water phase in all flumes as early as day 21. Since TP.VND was also the most frequently detected TP along with another abundant VEN TP (TP.VNO), we consider both as environmentally relevant. Similarly, in batch studies with activated sludge TP.VND increased over time, whereas the other venlafaxine TPs remained constant or decreased.[58] This observation is supported by the frequent occurrence of TP.VND in marine mussels[59] and the formation of TP.VNO as a major ozonation product of VEN.[60] We speculate that the occurrence of VEN metabolites may increase in surface waters with increasing implementation of wastewater ozonation.

https://dx.doi.org/10.1021/acs.est.9b06928
Environ. Sci. Technol. 2020, 54, 5467−5479

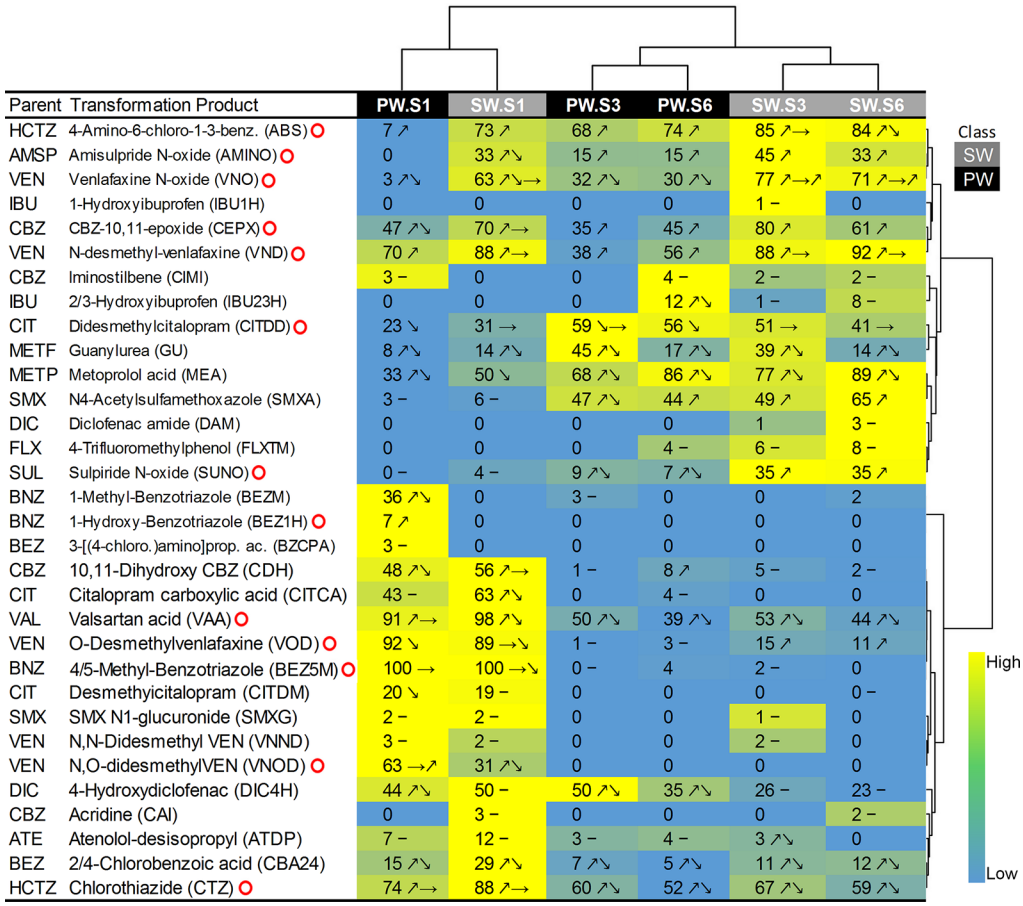

Figure 3. Heat map showing a two-way cluster analysis, using Euclidean distance measures with respect to detection rates (expressed as percent of all analyzed samples within the respective class with concentrations above the limit of quantification; fields were color coded with yellow denoting high detection rates and blue denoting low detection rates) of target transformation products (TPs) (Table SI.A-2). Hierarchical clusters were generated for TPs and average detection rates of the six sample classes (pore water (PW) or surface water (SW) for each of the three diversity levels as a function of sediment dilution: S1 (low dilution, high diversity), S3 (medium dilution/diversity), and S6 (high dilution, low diversity)). Observed TP concentration dynamics in surface water and pore water across the different bacterial diversities (*S*) are depicted as arrows: upward (↑), downward (↓), stable (→) concentration trends. Groups of arrows indicate cases in which changing trends were observed during the experiment. Dashes indicate cases where no clear trend was observed. Red circles indicate TPs that were identified as persistent in at least one of the classes. Five TPs were not detected in any sample and are therefore not shown: 4-hydroxy-1*H*-benzotriazole, acridone, diclofenac amide, carboxyibuprofen, *α*-hydroxymetoprolol.

A two-way cluster analysis using Euclidean distance measures was performed with respect to detection rates of target TPs, and hierarchical clusters were generated for sample type (pore water or surface water) and compounds (Figure 3). Pore and surface water of S1 treatments clustered together, while in S3 and S6 systems, the compartment (pore water, surface water) was more defining for the TP composition than the diversity level. Two main clusters were observed: one comprising 17 TPs that were primarily detected in both pore and surface water of the S1 flumes and a second smaller group of 15 TPs dominating in surface water of S levels 3 and 6. While the occurrence of group one TPs was largely limited to S1 flumes, TPs from the second group were also found in other S levels and pore water. Higher detection rates, concentrations, and longevity of TPs in S6 flumes can be explained with transformation pathways requiring several types of bacteria. A less diverse microbial community has a lower probability to host elements of such pathways, leading to enrichment of certain intermediates. TPs were least often detected in pore water of the high-diversity systems (S1), where we expect the most diverse bacterial communities and well-functioning transformation sequences. Thus, such data demonstrate the importance of microbial diversity and by extension a diverse gene pool translating into a high genetic potential and finally organic contaminant degradation potential in hyporheic zones.

3.6.1. Bacterial Diversity Drives Formation−Attenuation Dynamics of Metoprolol Acid. Atenolol and metoprolol are structurally similar beta-blockers that underwent complete attenuation (≥99% across all flumes) in ≤42 days (atenolol) and ≤28 days (metoprolol) (sections SI.H−SI.J). TP dynamics are summarized in Figure 3 and Table SI.M-22, whereas time trends of atenolol, metoprolol, and respective TPs are shown in section SI.M.e. A common and major TP is atenolol/metoprolol acid (Figure 4), which is formed from atenolol by (microbial) enzymatic hydrolysis,[61] from metoprolol through CYP450-mediated dealkylation during aerobic microbial biotransformation,[58] and in human metabolism.[58,62] Moreover, metoprolol acid has been reported to form from metoprolol in microalgae (*Haematococcus pluvialis*,[63] *Chlamydomonas reinhardtii*[64]), from atenolol in the cyanobacterium *Synechococcus* sp.,[64] from metoprolol by fungal treatment,[65] and by abiotic hydrolysis.[66] Since microalgae are a major

https://dx.doi.org/10.1021/acs.est.9b06928
Environ. Sci. Technol. 2020, 54, 5467−5479

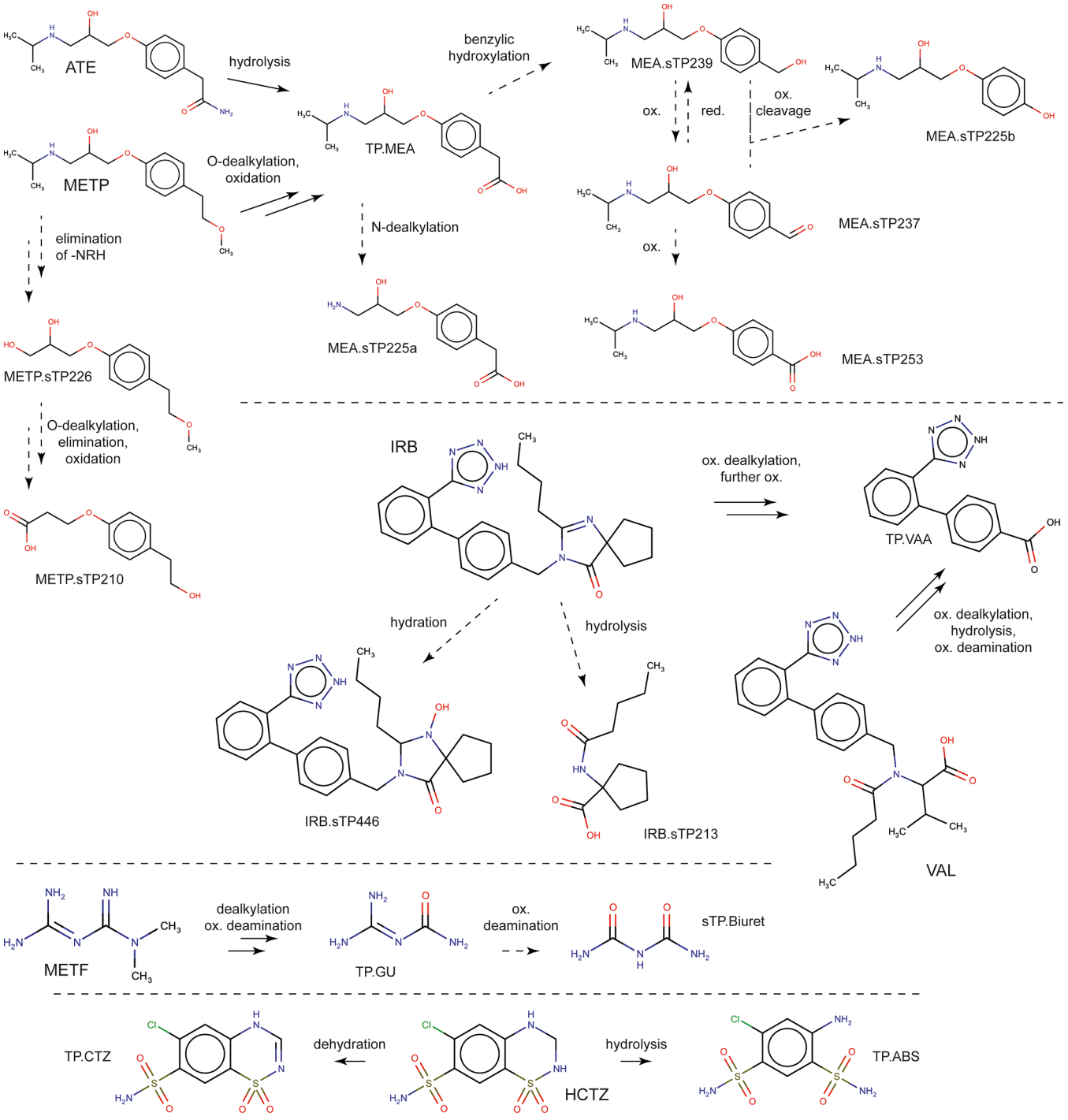

Figure 4. Proposed formation pathways for target transformation products (TP, solid lines) and tentatively identified (confidence level 3) suspect TPs (sTPs, dashed lines) of atenolol (ATE)/metoprolol (METP), hydrochlorothiazide (HCTZ, see section SI.M.g for a discussion), irbesartan (IRB)/valsartan (VAL), and metformin (METF). Metoprolol acid (MEA) pathways were adapted from ref 65. All compounds are depicted in their neutral form despite potential speciation at flume pH. Abbreviations: TP.VAA = valsartan acid, TP.GU = guanylurea. Please note that confidence level 3 of identification might allow multiple structural isomers and the displayed structures only display one possible but very likely isomer retrieved from the literature and/or predicted in silico (details in Table SI.M-22).

component of biofilms, and biofilm growth was observed in the majority of the flumes, biotransformation of atenolol/metoprolol in microalgae cannot be ruled out. In S6 and S3 flumes (low and medium diversity), metoprolol acid was more frequently detected and was at higher concentrations than in S1 flumes (low dilution, high diversity). This can be explained by the dissipation of metoprolol acid, which was faster with increasing bacterial diversity. Consequently, at the highest bacterial diversity (S1), metoprolol acid was only observed in traces and mostly during the first few days after fortification. In these treatments, it is likely that attenuation proceeded so fast that the sampling resolution was not sufficient to capture formation−attenuation dynamics. The biodegradability of metoprolol acid observed here is consistent with prior

https://dx.doi.org/10.1021/acs.est.9b06928
Environ. Sci. Technol. 2020, 54, 5467−5479

biodegradation studies,[11,58,63,65] some of which also reported metoprolol acid TPs[63,65] which were observed in surface water from the present study. The absence or fast dissipation of metoprolol acid in S1 flumes coincided with intense signals of MEA.sTP225a and MEA.sTP225b (Figure 4 and Section SI.M.e) at day 1, which subsequently decreased until day 7. In S3 flumes, MEA.sTP225a dynamics followed the trend of metoprolol acid (increase−decrease). In S1 flumes, the signal decrease of MEA.sTP225a and -226b was accompanied by a short pulse of MEA.sTP239 (increase from day 1 to day 3, decrease until day 14). In S3 and S6 flumes, the trend of MEA.sTP239 was similar to that of metoprolol acid (increase−decrease). The oxidation product MEA.sTP237 increased in all S1 flumes until day 28 and was then stable or only slowly decreased. MEA.TP253 did not show a clear pattern among the S1 flumes but peaked shortly after the drop of the metoprolol acid in S6 flumes. In summary, one TP was observed for atenolol, two TPs (plus 2 sTPs) were observed for metoprolol, and five sTPs were observed for metoprolol acid (Figure 4).

3.6.2. Further Evidence for the Formation of Valsartan Acid from Irbesartan. Irbesartan (log D_{ow} 4.0) and valsartan (log D_{ow} 0.3) are structurally similar antihypertensive drugs that differ in polarity and dissipated by >96% across all flumes. In the RSM, only the linear *S* term was significant for valsartan, explaining 77% of the DT50 variability: i.e., the attenuation of valsartan was mainly driven by bacterial diversity and DT50s were decreasing with increasing sediment dilution. In contrast, a strong initial concentration drop was observed for irbesartan, likely due to sorption, which impeded DT50 calculations and had a strong effect on the RSM fit (adjusted R2 of 0.095). Consequently, neither the *S* nor the *B* term could explain the DT50 variability for irbesartan. Median DT50s of both substances were similar (irbesartan, 7.3 days; valsartan, 7.6 days), although attenuation of irbesartan continued throughout the experiment. In all flumes, dissipation of valsartan and irbesartan was accompanied by formation of valsartan acid. Interestingly, valsartan acid concentrations steadily increased over 56 days (section SI.N) in surface and pore water, with an intermittent concentration drop at day 42 in S1 and S3 flumes (high and medium diversity). This drop was likely caused by the depletion of valsartan in all flumes before day 20 and a switch to formation from irbesartan, leading to increasing valsartan acid concentrations until day 56. The unique shape of the irbesartan RSM 3D plot (section SI.K.b) might be an outcome of this competition. The differences in attenuation between valsartan and irbesartan were less pronounced in S6 flumes (low diversity) and here we do not see the valsartan acid concentration drop at day 42 in surface water, which supports the hypothesis that both valsartan and irbesartan contribute to valsartan acid formation. Further evidence is the mass balance of valsartan acid, which shows higher molar concentrations of valsartan acid than can be formed from valsartan alone (valsartan acid measured average 4.44×10^{-8} M vs theoretically spiked concentration of valsartan 2.30×10^{-8} M + irbesartan $2.33 \times 10^{-8} = 4.63 \times 10^{-8}$ M). Valsartan acid levels dropped in the surface water of all flumes between day 56 and 78 by ∼50% (constant only in S1 pore water). Eventually, valsartan acid is further transformed, which is only observed after both parent compounds have been consumed and no more valsartan acid is delivered. Formation of valsartan acid from valsartan and irbesartan has also been described for a laboratory-scale WWTP, where turnover into valsartan acid accounted for 3.9 and 1 mol %, respectively.[67] Transformation of valsartan into valsartan acid starts with oxidative dealkylation at the tertiary amide group, which is followed by hydrolysis and oxidative deamination.[58,68] A pathway for the transformation of irbesartan into valsartan acid has not yet been proposed. According to the Eawag-Biocatalysis/Biodegradation Database Pathway Prediction System (section SI.C), irbesartan undergoes oxidative dealkylation (rule bt0243) into amide and aldehyde (valsartan acid precursor), followed by oxidation (rule bt003) of the aldehyde into valsartan acid (Figure 4). Although the transformation of valsartan involves three steps in comparison to only two steps in irbesartan, the noncyclic amide structure of valsartan might be more enzymatically accessible and preferably biotransformed. Irbesartan may also be less bioavailable. In earlier field studies in the River Erpe, increased levels of valsartan acid were observed in hyporheic pore water relative to surface water under downwelling conditions,[13,14] confirming the relevance of this TP in the environment.

3.6.3. Transformation Products of Metformin: Guanylurea and the Novel TP Biuret. We observed significant linear and quadratic effects of diversity on metformin attenuation (Figure 2 and section SI.K), while HEF had no significant effect. Depletion of metformin was driven by biotransformation, as shown by the formation and abundance of its main transformation product guanylurea, confirming previous studies.[52] Biuret (sTP103, sections SI.A, SI.M, and SI.N) was identified as a suspect TP with the highest intensities in S1 flumes (low dilution, high diversity) with B0 and B6. A biuret standard was acquired, and the suspected TP was successfully confirmed (confidence level 1) (see section SI.O). Guanylurea is formed by dealkylation and oxidative deamination of metformin at one of the two guanide groups,[69] yielding a carbonyl group. Biuret in turn might result from oxidative deamination of guanylurea, introducing a second carbonyl group (Figure 4), which is a biologically occurring process that might even involve the same enzyme facilitating part of the transformation from metformin to guanylurea.[70] To our knowledge, this compound has not been previously reported as a TP of metformin. Transformation of metformin to guanylurea occurs primarily within WWTPs.[71] Our prior work in the River Erpe reported a discharge ratio of ∼1:40 metformin:guanylurea from the local WWTP[17] with little attenuation observed for either compound.[33] However, the present data set suggests that the resident microbial community in Erpe sediments is capable of breaking down metformin and guanylurea, as both were fully attenuated under all types of flume conditions (section SI.N). According to the literature, this attenuation cannot be attributed to direct photolysis.[69] A maximum concentration of 9 $\mu g\ L^{-1}$ of guanylurea was measured in surface water of flume 5 (S3 B0, medium diversity) after 21 days (Table SI.M-20). Here we can assume complete transformation from metformin (guanylurea 8.8×10^{-8} M in comparison to the nominally spiked metformin 7.7×10^{-8} M). Interestingly, guanylurea was also found at substantially higher average concentrations in surface and pore water of S3 flumes (1.1 and 1.2 $\mu g\ L^{-1}$) in comparison to those with S1 (0.06 and 0.08 $\mu g\ L^{-1}$) and S6 (low) diversity (0.1 and 0.2 $\mu g\ L^{-1}$). In batch experiments, it was repeatedly observed that metformin transformation is highly variable and may be strongly dependent on the exact composition of bacterial communities,[69] which would explain our observation. The genus *Mesorhizobium*, which has been

https://dx.doi.org/10.1021/acs.est.9b06928
Environ. Sci. Technol. 2020, 54, 5467−5479

previously identified as degraders of metformin,[52] exhibited a negative $\log_2$ fold change (−1.6) in S1 treatments but a positive $\log_2$ fold change (3.5) in S6 flumes relative to unamended controls. A direct comparison of diversity levels revealed significantly higher abundance of *Mesorhizobium* in S3 and S6 relative to S1 but only insignificant differences between S3 and S6 ($\log_2$ fold change: S1 vs S3 = 1.6; S1 vs S6 = 1.8; $p < 0.01$), which does not match the observed degradation dynamics of metformin and guanylurea, and thus there must be other bacterial strains involved. Averaged guanylurea concentrations were lower in B6 flumes in comparison to B3 and B0 at most time points. Guanylurea has been shown to be degraded in hyporheic sediments,[2] but increased sorption of the cationic species at flume pH (low log D_{ow} of −3.4) and better contact with binding sites in high HEF flumes[72] might also be an explanation. This is supported by the fact that retardation of both metformin and guanylurea has been observed in situ in the river Erpe sediment.[2]

4. ENVIRONMENTAL IMPLICATIONS

While bacterial diversity influenced the biotransformation of 20 substances, only acesulfame, ibuprofen, sitagliptin, and metaxalone were significantly influenced by HEF. This may imply that the last four substances are particularly sensitive to biodegradation in hyporheic zones. Interestingly, ibuprofen and metaxalone degraded to a lesser extent with increasing number of bedforms, which contrasts the hypothesis that hyporheic exchange generally increases degradation potential. A common characteristic of acesulfame, ibuprofen, and sitagliptin is that they have all been previously reported to undergo redox reactions.[7,73,74] Little information about the environmental fate of metaxalone is available. Hence, the bedforms might have provided a particular redox environment that favored or diminished transformation reactions of those aforementioned compounds. However, the fact that degradation of other redox-sensitive compounds, such as the beta-blockers metoprolol, atenolol, and sotalol,[75] was not significantly influenced by the number of bedforms highlights the complexity of compound-specific reactions. As discussed previously for acesulfame,[31] the absence of a visible effect of HEF may also be caused by the pronounced effect of the diversity treatment, which ultimately masks the influence of HEF. Some compounds show differences among bedform treatments within the lowest diversity, but this effect is not significant in the overall model because the differences vanish in the higher diversity treatments (e.g., METP, ATE, BEZ, GEM, VAL). Alternatively, differences in HEF levels were not sufficient to observe a significant effect on DT50s in the RSMs of the other 20 substances. Although a numerical model[34] shows that the bedform treatments differ in HEF, these differences were diminished by the effects of bedforms on the flow velocities of the overlying water. In future studies, larger differences in HEF would likely result in more distinct dramatic effects of HEF on more compounds. This might be achieved by a numerical model that predicts the highest possible HEF variation for an experimental setup. Still, even if the differences are increased, HEF alone will likely not be a perfect predictor of degradation, as hyporheic travel time distributions and associated redox zonation as well as variations in microbial communities along flow paths will differ with HEF and therefore should always be taken into account. The number, type, and quantity of formed target and suspect TPs align well with our interpretation of parent compound DT50s. TP.VND was not only the most frequently detected target TP but also the only compound which persisted across all treatment groups and compartments. Taxa enriched in the presence of organic contaminants relative to unamended controls included uncultured Acidobacteria, Sphingomonadaceae, Pseudomonadaceae, Nocardioides spp., Illumatobacter spp., and many uncultured/unclassified taxa, suggesting a potential contribution of such taxa to biotransformation processes in the hyporheic zone. Collectively, these data demonstrate the importance of bacterial diversity and HEF on the biotransformation of organic contaminants and highlight hyporheic zones as reservoirs of new microbial diversity. Since both bacteria and eukaryotes may play a role in contaminant biodegradation, we suggest to include both in taxonomic analysis (18 sRNA). In addition, analysis of the metatranscriptome (expressed metabolic genes) may help explain concentration dynamics, as it indicates not only the abundance but also the activity of species. Restoration measures designed to increase HEF tend to increase the reactivity of organic contaminants on the reach scale and the efficiency of rivers toward contaminant removal.[3] On the basis of our findings, we further conclude that restoration measures promoting microbial diversity which might require novel concepts, protection measures, and change of land use within the reach[68] will further stimulate the in-stream removal capacity of rivers.

■ ASSOCIATED CONTENT

Supporting Information

The Supporting Information is available free of charge at https://pubs.acs.org/doi/10.1021/acs.est.9b06928.

Compound properties and supplier information, details of the experimental design, setup, and timeline. details of the instrumental analysis and method comparison, details of the bacterial analysis, statistics, and results, dissipation half-lives, detailed information on the RSM, 3D plots, coefficients, and significance, background concentration data for blank flumes, details on transformation product analysis, targets, and suspects; ,and concentration time trends (PDF)

■ AUTHOR INFORMATION

Corresponding Authors

Marcus A. Horn − *Department of Ecological Microbiology, University of Bayreuth, Bayreuth, Germany; Institute of Microbiology, Leibniz University of Hannover, DE-30167 Hannover, Germany*; Email: horn@ifmb.uni-hannover.de

Juliane Hollender − *Eawag, Swiss Federal Institute of Aquatic Science and Technology, CH 8600 Dübendorf, Switzerland; Institute of Biogeochemistry and Pollutant Dynamics, ETH Zurich, 8092 Zürich, Switzerland*; orcid.org/0000-0002-4660-274X; Email: juliane.hollender@eawag.ch

Jonathan P. Benskin − *Department of Environmental Science (ACES), Stockholm University, SE-11418 Stockholm, Sweden*; Email: jon.benskin@aces.su.se

Authors

Malte Posselt − *Department of Environmental Science (ACES), Stockholm University, SE-11418 Stockholm, Sweden*; orcid.org/0000-0001-8979-8044

Jonas Mechelke − *Eawag, Swiss Federal Institute of Aquatic Science and Technology, CH 8600 Dübendorf, Switzerland;*

https://dx.doi.org/10.1021/acs.est.9b06928
Environ. Sci. Technol. 2020, 54, 5467−5479

Institute of Biogeochemistry and Pollutant Dynamics, ETH Zurich, 8092 Zürich, Switzerland

Cyrus Rutere − *Department of Ecological Microbiology, University of Bayreuth, Bayreuth, Germany*

Claudia Coll − *Department of Environmental Science (ACES), Stockholm University, SE-11418 Stockholm, Sweden; Eawag, Swiss Federal Institute of Aquatic Science and Technology, CH 8600 Dübendorf, Switzerland;* orcid.org/0000-0003-1100-1263

Anna Jaeger − *Department Ecohydrology, Leibniz-Institute of Freshwater Ecology and Inland Fisheries, Berlin, Germany; Geography Department, Humboldt University Berlin, Berlin, Germany;* orcid.org/0000-0002-9141-3235

Muhammad Raza − *Technical University of Darmstadt, Institute of Applied Geosciences, Darmstadt, Germany; IWW Water Centre, Mülheim an der Ruhr, Germany*

Karin Meinikmann − *Department Ecohydrology, Leibniz-Institute of Freshwater Ecology and Inland Fisheries, Berlin, Germany; Julius Kühn-Institute, Institute for Ecological Chemistry, Plant Analysis and Stored Product Protection, Berlin, Germany*

Stefan Krause − *School of Geography, Earth and Environmental Sciences, University of Birmingham, Birmingham, U.K.*

Anna Sobek − *Department of Environmental Science (ACES), Stockholm University, SE-11418 Stockholm, Sweden;* orcid.org/0000-0002-1549-7449

Jörg Lewandowski − *Department Ecohydrology, Leibniz-Institute of Freshwater Ecology and Inland Fisheries, Berlin, Germany; Geography Department, Humboldt University Berlin, Berlin, Germany*

Complete contact information is available at: https://pubs.acs.org/10.1021/acs.est.9b06928

Author Contributions

△M.P., J.M., and C.R. contributed equally to the paper.

Author Contributions

◇M.A.H., J.H., and J.P.B. share the last authorship.

Funding

This project has received funding from the European Union's Horizon 2020 research and innovation program under the Marie Sklodowska-Curie grant agreement No. 641939 and the Swiss State Secretariat for Education, Research and Innovation.

Notes

The authors declare no competing financial interest.

■ ACKNOWLEDGMENTS

We thankfully acknowledge help by all HypoTRAIN ESRs and supervisors involved in the flume experiment, and especially Andrea Betterle (Eawag), Anne Mehrtens (University of Oldenburg), Andrea Portmann (Colorado School of Mines), and Tanu Singh and Phillip Blaen (University of Birmingham). This experiment was only made possible with many helping hands and was a result of excellent collaboration before, during, and after the study at the University of Birmingham and the support of their Environmental Change Outdoor Laboratory. Finally, we gratefully acknowledge ChemAxon Ltd. for the donation of an academic research license to the JChem package.

■ REFERENCES

(1) Margot, J.; Rossi, L.; Barry, D. A.; Holliger, C. A review of the fate of micropollutants in wastewater treatment plants. *Wiley Interdiscip. Rev.: Water* **2015**, *2* (5), 457−487.

(2) Schaper, J. L.; Posselt, M.; Bouchez, C.; Jaeger, A.; Nuetzmann, G.; Putschew, A.; Singer, G.; Lewandowski, J. Fate of Trace Organic Compounds in the Hyporheic Zone: Influence of Retardation, the Benthic Biolayer, and Organic Carbon. *Environ. Sci. Technol.* **2019**, *53* (8), 4224−4234.

(3) Schaper, J. L.; Posselt, M.; McCallum, J. L.; Banks, E. W.; Hoehne, A.; Meinikmann, K.; Shanafield, M. A.; Batelaan, O.; Lewandowski, J. Hyporheic Exchange Controls Fate of Trace Organic Compounds in an Urban Stream. *Environ. Sci. Technol.* **2018**, *52* (21), 12285−12294.

(4) Battin, T. J.; Besemer, K.; Bengtsson, M. M.; Romani, A. M.; Packmann, A. I. The ecology and biogeochemistry of stream biofilms. *Nat. Rev. Microbiol.* **2016**, *14* (4), 251.

(5) Baschien, C.; Manz, W.; Neu, T. R.; Marvanová, L.; Szewzyk, U. In situ detection of freshwater fungi in an alpine stream by new taxon-specific fluorescence in situ hybridization probes. *Appl. Environ. Microbiol.* **2008**, *74* (20), 6427−6436.

(6) Buriánková, I.; Brablcová, L.; Mach, V.; Dvořák, P.; Chaudhary, P. P.; Rulík, M. Identification of methanogenic archaea in the hyporheic sediment of Sitka stream. *PLoS One* **2013**, *8* (11), e80804.

(7) Burke, V.; Greskowiak, J.; Asmuß, T.; Bremermann, R.; Taute, T.; Massmann, G. Temperature dependent redox zonation and attenuation of wastewater-derived organic micropollutants in the hyporheic zone. *Sci. Total Environ.* **2014**, *482*, 53−61.

(8) Löffler, D.; Römbke, J.; Meller, M.; Ternes, T. A. Environmental Fate of Pharmaceuticals in Water/Sediment Systems. *Environ. Sci. Technol.* **2005**, *39* (14), 5209−5218.

(9) Radke, M.; Lauwigi, C.; Heinkele, G.; Mürdter, T. E.; Letzel, M. Fate of the Antibiotic Sulfamethoxazole and Its Two Major Human Metabolites in a Water Sediment Test. *Environ. Sci. Technol.* **2009**, *43* (9), 3135−3141.

(10) Radke, M.; Maier, M. P. Lessons learned from water/sediment-testing of pharmaceuticals. *Water Res.* **2014**, *55*, 63−73.

(11) Li, Z.; Maier, M. P.; Radke, M. Screening for pharmaceutical transformation products formed in river sediment by combining ultrahigh performance liquid chromatography/high resolution mass spectrometry with a rapid data-processing method. *Anal. Chim. Acta* **2014**, *810*, 61−70.

(12) Radke, M.; Ulrich, H.; Wurm, C.; Kunkel, U. Dynamics and attenuation of acidic pharmaceuticals along a river stretch. *Environ. Sci. Technol.* **2010**, *44* (8), 2968−2974.

(13) Kunkel, U.; Radke, M. Reactive tracer test to evaluate the fate of pharmaceuticals in rivers. *Environ. Sci. Technol.* **2011**, *45* (15), 6296−6302.

(14) Kunkel, U.; Radke, M. Fate of pharmaceuticals in rivers: deriving a benchmark dataset at favorable attenuation conditions. *Water Res.* **2012**, *46* (17), 5551−5565.

(15) Lewandowski, J.; Putschew, A.; Schwesig, D.; Neumann, C.; Radke, M. Fate of organic micropollutants in the hyporheic zone of a eutrophic lowland stream: Results of a preliminary field study. *Sci. Total Environ.* **2011**, *409* (10), 1824−1835.

(16) Schaper, J. L.; Seher, W.; Nützmann, G.; Putschew, A.; Jekel, M.; Lewandowski, J. The fate of polar trace organic compounds in the hyporheic zone. *Water Res.* **2018**, *140*, 158−166.

(17) Posselt, M.; Jaeger, A.; Schaper, J. L.; Radke, M.; Benskin, J. P. Determination of polar organic micropollutants in surface and pore water by high-resolution sampling-direct injection-ultra high performance liquid chromatography-tandem mass spectrometry. *Environmental Science: Processes & Impacts* **2018**, *20* (12), 1716−1727.

(18) Mechelke, J.; Vermeirssen, E. L. M.; Hollender, J. Passive sampling of organic contaminants across the water-sediment interface of an urban stream. *Water Res.* **2019**, *165*, 114966.

(19) Andrés-Costa, M. J.; Proctor, K.; Sabatini, M. T.; Gee, A. P.; Lewis, S. E.; Pico, Y.; Kasprzyk-Hordern, B. Enantioselective

transformation of fluoxetine in water and its ecotoxicological relevance. *Sci. Rep.* **2017**, *7* (1), 1.
(20) Nałęcz-Jawecki, G. In Vitro Biotransformation of Amitriptyline and Imipramine with Rat Hepatic S9 Fraction: Evaluation of the Toxicity with Spirotox and Thamnotoxkit F Tests. *Arch. Environ. Contam. Toxicol.* **2008**, *54* (2), 266−273.
(21) Quintana, J.; Weiss, S.; Reemtsma, T. Pathways and metabolites of microbial degradation of selected acidic pharmaceutical and their occurrence in municipal wastewater treated by a membrane bioreactor. *Water Res.* **2005**, *39* (12), 2654−2664.
(22) Abellán, M. N.; Bayarri, B.; Giménez, J.; Costa, J. Photocatalytic degradation of sulfamethoxazole in aqueous suspension of TiO2. *Appl. Catal., B* **2007**, *74* (3−4), 233−241.
(23) Reemtsma, T.; Berger, U.; Arp, H. P. H.; Gallard, H.; Knepper, T. P.; Neumann, M.; Quintana, J. B.; Voogt, P. d. Mind the Gap: Persistent and Mobile Organic Compounds—Water Contaminants That Slip Through. *Environ. Sci. Technol.* **2016**, *50* (19), 10308−10315.
(24) Boxall, A. B. A.; Sinclair, C. J.; Fenner, K.; Kolpin, D.; Maund, S. J. Peer Reviewed: When Synthetic Chemicals Degrade in the Environment. *Environ. Sci. Technol.* **2004**, *38* (19), 368A−375A.
(25) Hollender, J.; Schymanski, E. L.; Singer, H. P.; Ferguson, P. L. Nontarget Screening with High Resolution Mass Spectrometry in the Environment: Ready to Go? *Environ. Sci. Technol.* **2017**, *51* (20), 11505−11512.
(26) Krauss, M.; Singer, H.; Hollender, J. LC−high resolution MS in environmental analysis: from target screening to the identification of unknowns. *Anal. Bioanal. Chem.* **2010**, *397* (3), 943−951.
(27) Peter, K. T.; Herzog, S.; Tian, Z.; Wu, C.; McCray, J. E.; Lynch, K.; Kolodziej, E. P. Evaluating emerging organic contaminant removal in an engineered hyporheic zone using high resolution mass spectrometry. *Water Res.* **2019**, *150*, 140−152.
(28) Patsch, D.; Vliet, S.; Marcantini, L. G.; Johnson, D. R. Generality of associations between biological richness and the rates of metabolic processes across microbial communities. *Environ. Microbiol.* **2018**, *20* (12), 4356−4368.
(29) Hester, E.; Young, K.; Widdowson, M. Mixing of surface and groundwater induced by riverbed dunes: Implications for hyporheic zone definitions and pollutant reactions. *Water Resour. Res.* **2013**, *49* (9), 5221−5237.
(30) Peralta-Maraver, I.; Perkins, D. M.; Thompson, M. S. A.; Fussmann, K.; Reiss, J.; Robertson, A. L. Comparing biotic drivers of litter breakdown across stream compartments. *J. Anim. Ecol.* **2019**, *88* (8), 1146−1157.
(31) Jaeger, A.; Coll, C.; Posselt, M.; Mechelke, J.; Rutere, C.; Betterle, A.; Raza, M.; Mehrtens, A.; Meinikmann, K.; Portmann, A. Using recirculating flumes and a response surface model to investigate the role of hyporheic exchange and bacterial diversity on micropollutant half-lives. *Environmental Science: Processes & Impacts* **2019**, *21* (12), 2093−2108.
(32) Stadler, L. B.; Delgado Vela, J.; Jain, S.; Dick, G. J.; Love, N. G. Elucidating the impact of microbial community biodiversity on pharmaceutical biotransformation during wastewater treatment. *Microb. Biotechnol.* **2018**, *11* (6), 995−1007.
(33) Jaeger, A.; Posselt, M.; Betterle, A.; Schaper, J.; Mechelke, J.; Coll, C.; Lewandowski, J. Spatial and Temporal Variability in Attenuation of Polar Organic Micropollutants in an Urban Lowland Stream. *Environ. Sci. Technol.* **2019**, *53* (5), 2383−2395.
(34) Betterle, A.; Jaeger, A.; Posselt, M.; Coll, C.; Benskin, J.; Schirmer, M. Analysis of Hyporheic Exchange Fluxes in Recirculating Flumes under Heterogeneous Microbial and Morphological Conditions. *Submitted Manuscript*, 2020.
(35) Kay, P.; Hughes, S. R.; Ault, J. R.; Ashcroft, A. E.; Brown, L. E. Widespread, routine occurrence of pharmaceuticals in sewage effluent, combined sewer overflows and receiving waters. *Environ. Pollut.* **2017**, *220*, 1447−1455.
(36) Paíga, P.; Correia, M.; Fernandes, M. J.; Silva, A.; Carvalho, M.; Vieira, J.; Jorge, S.; Silva, J. G.; Freire, C.; Delerue-Matos, C. Assessment of 83 pharmaceuticals in WWTP influent and effluent samples by UHPLC-MS/MS: Hourly variation. *Sci. Total Environ.* **2019**, *648*, 582−600.
(37) Xia, J.; Sinelnikov, I. V.; Han, B.; Wishart, D. S. MetaboAnalyst 3.0—making metabolomics more meaningful. *Nucleic Acids Res.* **2015**, *43* (W1), W251−W257.
(38) Schymanski, E. L.; Jeon, J.; Gulde, R.; Fenner, K.; Ruff, M.; Singer, H. P.; Hollender, J. Identifying small molecules via high resolution mass spectrometry: communicating confidence. *Environ. Sci. Technol.* **2014**, *48*, 2097.
(39) Ranke, J.; Lindenberger, K.; Lehmann, R.; Ag, E. R.; Ranke, M. J. *Package "mkin"*; 2020.
(40) Team, R. C. *R: A language and environment for statistical computing*; 2013.
(41) Lenth, R. V. *Package "rsm" Ver. 2.10*; 2018.
(42) Love, M. I.; Huber, W.; Anders, S. Moderated estimation of fold change and dispersion for RNA-seq data with DESeq2. *Genome Biol.* **2014**, *15* (12), 550.
(43) Triska, F. J.; Kennedy, V. C.; Avanzino, R. J.; Zellweger, G. W.; Bencala, K. E. Retention and Transport of Nutrients in a Third-Order Stream in Northwestern California: Hyporheic Processes. *Ecology* **1989**, *70* (6), 1893−1905.
(44) Nogales, B.; Moore, E. R. B.; Abraham, W.-R.; Timmis, K. N. Identification of the metabolically active members of a bacterial community in a polychlorinated biphenyl-polluted moorland soil. *Environ. Microbiol.* **1999**, *1* (3), 199−212.
(45) George, I. F.; Liles, M. R.; Hartmann, M.; Ludwig, W.; Goodman, R. M.; Agathos, S. N. Changes in soilAcidobacteriacommunities after 2,4,6-trinitrotoluene contamination. *FEMS Microbiol. Lett.* **2009**, *296* (2), 159−166.
(46) Chen, Y. J.; Rosazza, J. P. N. A Bacterial, Nitric Oxide Synthase from a Nocardia Species. *Biochem. Biophys. Res. Commun.* **1994**, *203* (2), 1251−1258.
(47) Rodríguez, J.; Gallampois, C. M. J.; Timonen, S.; Andersson, A.; Sinkko, H.; Haglund, P.; Berglund, Å. M. M.; Ripszam, M.; Figueroa, D.; Tysklind, M.; Rowe, O. Effects of Organic Pollutants on Bacterial Communities Under Future Climate Change Scenarios. *Front. Microbiol.* **2018**, *9*, 1.
(48) Song, M.; Luo, C.; Jiang, L.; Zhang, D.; Wang, Y.; Zhang, G. Identification of Benzo[a]pyrene-Metabolizing Bacteria in Forest Soils by Using DNA-Based Stable-Isotope Probing. *Appl. Environ. Microbiol.* **2015**, *81* (21), 7368−7376.
(49) Li, Y.; Wu, B.; Zhu, G.; Liu, Y.; Ng, W. J.; Appan, A.; Tan, S. K. High-throughput pyrosequencing analysis of bacteria relevant to cometabolic and metabolic degradation of ibuprofen in horizontal subsurface flow constructed wetlands. *Sci. Total Environ.* **2016**, *562*, 604−613.
(50) Ghosal, D.; Ghosh, S.; Dutta, T. K.; Ahn, Y. Corrigendum: Current State of Knowledge in Microbial Degradation of Polycyclic Aromatic Hydrocarbons (PAHs): A Review. *Front. Microbiol.* **2016**, *7*, 1.
(51) Dallinger, A.; Horn, M. A. Agricultural soil and drilosphere as reservoirs of new and unusual assimilators of 2,4-dichlorophenol carbon. *Environ. Microbiol.* **2014**, *16* (1), 84−100.
(52) Poursat, B. A.; van Spanning, R. J.; Braster, M.; Helmus, R.; de Voogt, P.; Parsons, J. R. Biodegradation of metformin and its transformation product, guanylurea, by natural and exposed microbial communities. *Ecotoxicol. Environ. Saf.* **2019**, *182*, 109414.
(53) T'Syen, J.; Tassoni, R.; Hansen, L.; Sorensen, S. J.; Leroy, B.; Sekhar, A.; Wattiez, R.; De Mot, R.; Springael, D. Identification of the Amidase BbdA That Initiates Biodegradation of the Groundwater Micropollutant 2,6-dichlorobenzamide (BAM) in Aminobacter sp. MSH1. *Environ. Sci. Technol.* **2015**, *49* (19), 11703−11713.
(54) Lawrence, J. R.; Swerhone, G. D.; Wassenaar, L. I.; Neu, T. R. Effects of selected pharmaceuticals on riverine biofilm communities. *Can. J. Microbiol.* **2005**, *51* (8), 655−669.
(55) Schaffer, M.; Börnick, H.; Nödler, K.; Licha, T.; Worch, E. Role of cation exchange processes on the sorption influenced transport of cationic β-blockers in aquifer sediments. *Water Res.* **2012**, *46* (17), 5472−5482.

https://dx.doi.org/10.1021/acs.est.9b06928
Environ. Sci. Technol. 2020, 54, 5467−5479

(56) Johnson, D. R.; Helbling, D. E.; Lee, T. K.; Park, J.; Fenner, K.; Kohler, H.-P. E.; Ackermann, M. Association of Biodiversity with the Rates of Micropollutant Biotransformations among Full-Scale Wastewater Treatment Plant Communities. *Appl. Environ. Microbiol.* **2015**, *81* (2), 666−675.
(57) Huntscha, S.; Hofstetter, T. B.; Schymanski, E. L.; Spahr, S.; Hollender, J. Biotransformation of benzotriazoles, insights from transformation product identification and compound-specific isotope analysis. *Environ. Sci. Technol.* **2014**, *48*, 4435.
(58) Kern, S.; Baumgartner, R.; Helbling, D. E.; Hollender, J.; Singer, H.; Loos, M. J.; Schwarzenbach, R. P.; Fenner, K. A tiered procedure for assessing the formation of biotransformation products of pharmaceuticals and biocides during activated sludge treatment. *J. Environ. Monit.* **2010**, *12* (11), 2100.
(59) Martínez Bueno, M. J.; Boillot, C.; Munaron, D.; Fenet, H.; Casellas, C.; Gómez, E. Occurrence of venlafaxine residues and its metabolites in marine mussels at trace levels: development of analytical method and a monitoring program. *Anal. Bioanal. Chem.* **2014**, *406* (2), 601−610.
(60) Zucker, I.; Mamane, H.; Riani, A.; Gozlan, I.; Avisar, D. Formation and degradation of N-oxide venlafaxine during ozonation and biological post-treatment. *Sci. Total Environ.* **2018**, *619−620*, 578−586.
(61) Radjenović, J.; Pérez, S.; Petrović, M.; Barceló, D. Identification and structural characterization of biodegradation products of atenolol and glibenclamide by liquid chromatography coupled to hybrid quadrupole time-of-flight and quadrupole ion trap mass spectrometry. *Journal of Chromatography A* **2008**, *1210* (2), 142−153.
(62) Rubirola, A.; Llorca, M.; Rodriguez-Mozaz, S.; Casas, N.; Rodriguez-Roda, I.; Barceló, D.; Buttiglieri, G. Characterization of metoprolol biodegradation and its transformation products generated in activated sludge batch experiments and in full scale WWTPs. *Water Res.* **2014**, *63*, 21−32.
(63) Lv, M.; Lo, C.; Hsu, C.-C.; Wang, Y.; Chiang, Y.-R.; Sun, Q.; Wu, Y.; Li, Y.; Chen, L.; Yu, C.-P. Identification of Enantiomeric Byproducts During Microalgae-Mediated Transformation of Metoprolol by MS/MS Spectrum Based Networking. *Front. Microbiol.* **2018**, *9*, 1.
(64) Stravs, M. A.; Pomati, F.; Hollender, J. Exploring micropollutant biotransformation in three freshwater phytoplankton species. *Environmental Science: Processes & Impacts* **2017**, *19* (6), 822−832.
(65) Jaén-Gil, A.; Castellet-Rovira, F.; Llorca, M.; Villagrasa, M.; Sarrà, M.; Rodríguez-Mozaz, S.; Barceló, D. Fungal treatment of metoprolol and its recalcitrant metabolite metoprolol acid in hospital wastewater: Biotransformation, sorption and ecotoxicological impact. *Water Res.* **2019**, *152*, 171−180.
(66) Yin, L.; Ma, R.; Wang, B.; Yuan, H.; Yu, G. The degradation and persistence of five pharmaceuticals in an artificial climate incubator during a one year period. *RSC Adv.* **2017**, *7* (14), 8280−8287.
(67) Letzel, T.; Bayer, A.; Schulz, W.; Heermann, A.; Lucke, T.; Greco, G.; Grosse, S.; Schüssler, W.; Sengl, M.; Letzel, M. LC−MS screening techniques for wastewater analysis and analytical data handling strategies: Sartans and their transformation products as an example. *Chemosphere* **2015**, *137*, 198−206.
(68) Helbling, D. E.; Hollender, J.; Kohler, H.-P. E.; Singer, H.; Fenner, K. High-throughput identification of microbial transformation products of organic micropollutants. *Environ. Sci. Technol.* **2010**, *44* (17), 6621−6627.
(69) Trautwein, C.; Kümmerer, K. Incomplete aerobic degradation of the antidiabetic drug Metformin and identification of the bacterial dead-end transformation product Guanylurea. *Chemosphere* **2011**, *85* (5), 765−773.
(70) Arora, P. K. Bacterial degradation of monocyclic aromatic amines. *Front. Microbiol.* **2015**, *6*, 820.
(71) Trautwein, C.; Berset, J.-D.; Wolschke, H.; Kümmerer, K. Occurrence of the antidiabetic drug Metformin and its ultimate transformation product Guanylurea in several compartments of the aquatic cycle. *Environ. Int.* **2014**, *70*, 203−212.
(72) Briones, R. M.; Sarmah, A. K. Detailed sorption characteristics of the anti-diabetic drug metformin and its transformation product guanylurea in agricultural soils. *Sci. Total Environ.* **2018**, *630*, 1258−1268.
(73) Jia, Y.; Yin, L.; Khanal, S. K.; Zhang, H.; Oberoi, A. S.; Lu, H. Biotransformation of ibuprofen in biological sludge systems: Investigation of performance and mechanisms. *Water Res.* **2020**, *170*, 115303.
(74) Henning, N.; Falås, P.; Castronovo, S.; Jewell, K. S.; Bester, K.; Ternes, T. A.; Wick, A. Biological transformation of fexofenadine and sitagliptin by carrier-attached biomass and suspended sludge from a hybrid moving bed biofilm reactor. *Water Res.* **2019**, *167*, 115034.
(75) Schmidt, N.; Page, D.; Tiehm, A. Biodegradation of pharmaceuticals and endocrine disruptors with oxygen, nitrate, manganese (IV), iron (III) and sulfate as electron acceptors. *J. Contam. Hydrol.* **2017**, *203*, 62−69.

https://dx.doi.org/10.1021/acs.est.9b06928
Environ. Sci. Technol. 2020, 54, 5467−5479